Electronic topological and structural transitions in $AuGa_2$ under pressure

2006 J. Phys.: Condens. Matter 18 8523

(http://iopscience.iop.org/0953-8984/18/37/010)

INSTITUTE OF PHYSICS PUBLISHING JOURNAL OF PHYSICS: CONDENSED MATTER

J. Phys.: Condens. Matter **18** (2006) 8523–8532 doi:10.1088/0953-8984/18/37/010

Electronic topological and structural transitions in $AuGa_2$ under pressure

Alka B Garg[1], Ashok K Verma[1], V Vijayakumar[1], R S Rao[2] and B K Godwal[1]

[1] High Pressure Physics Division, Purnima Laboratories, Bhabha Atomic Research Centre, Mumbai 400085, India
[2] Laser and Neutron Physics Section, Purnima Laboratories, Bhabha Atomic Research Centre, Mumbai 400085, India

Received 29 March 2006, in final form 1 August 2006
Published 1 September 2006
Online at stacks.iop.org/JPhysCM/18/8523

Abstract

Results of electronic band structure calculations, electrical resistance, thermoelectric power (TEP), and x-ray diffraction measurements, under pressure carried out on $AuGa_2$ to investigate its anomalous behaviour are reported. The first principles electronic band structure calculations confirm that a flat band close to the Fermi level along the Γ–X direction of the Brillouin zone is responsible for the unusual behaviour of $AuGa_2$. In synchrotron-based high-pressure x-ray diffraction measurements, it is observed to undergo a structural phase transition above 7 GPa. The TEP variation with pressure and the P–V data up to 7 GPa transformed to the universal equation of state (UEOS) indicate the existence of an electronic topological transition (ETT) near 3.2 GPa. Consistent with this, in electronic structure calculations carried out at reduced sample volume corresponding to 4 GPa, it is seen that the flat band crosses the Fermi level. The structure above 7 GPa is a distortion of the CaF_2 phase. This structure continuously evolves with increasing pressure. The continuous variation of electrical resistance across the transition is consistent with this.

1. Introduction

Among the AuX_2 (X = Al, In, Ga) type intermetallics with CaF_2 structure, $AuGa_2$ is unique. The temperature variation of the thermoelectric power (TEP) of these three compounds exhibits a positive maximum in the temperature region corresponding to 0.2–0.25 θ_d (θ_d, Debye temperature). While the TEP of $AuIn_2$ and $AuAl_2$ remains positive from liquid helium to ambient temperature, that of $AuGa_2$ changes sign twice (at the lower and higher side of the above maximum) and has a low negative (-1.5 μV K^{-1}) value near 300 K [1]. $AuGa_2$ is the only nonmagnetic material to show a Knight shift that changes sign as a function of temperature [2]. The static magnetic susceptibility of $AuGa_2$ is also strongly temperature dependent. In contrast, isoelectronic $AuAl_2$ and $AuIn_2$ intermetallics have temperature-independent Knight shifts and susceptibilities [2, 3]. The temperature dependence of the

elastic constants of $AuGa_2$ also shows anomalous behaviour. This is clearly seen in the logarithmic temperature derivative of the elastic moduli C_{11} and C_{12}, which show anomalously large negative values near 85 K and strong temperature dependence [4]. Thus the details of electron occupancy and its variation with temperature and volume change of these materials have attracted considerable attention and have been investigated, both computationally [5] and experimentally [6, 7].

The electronic structure of these intermetallics is excellent for studying d-band evolution, as the Au separation in them is larger than in pure elements, making the d bands more localized. It is generally understood that the group III metals will enhance the conduction electron density by contributing s–p states to the valence band. In fact they are good metallic conductors and have specific applications; $AuAl_2$ is a selective solar absorber [8] and $AuGa_2$ has important usages in electronic circuitry [9]. $AuIn_2$ and $AuAl_2$ are type-I superconductors with T_c of 207 and 160 mK respectively [10].

Earlier non-relativistic augmented plane wave (APW) band structure calculations [5] on AuX_2 revealed the presence of an unusually flat band along the Γ–X direction of the Brillouin zone. It was also suggested that this band is derived from X s and Au d states [5]. The position of this band is just below the Fermi level in $AuGa_2$ and the band can get depopulated under thermal excitation or cross the Fermi level on a small volume reduction [2]. Thus $AuGa_2$ should exhibit interesting structural and electronic behaviour under high pressure. The measurement of the melting point variation with pressure on AuX_2 (X = In, Ga and Al) [11] shows that it exhibits a change of slope at 3 and 4 GPa for $AuIn_2$ and $AuGa_2$ respectively, implying an electronic or structural transition in them in the above pressure regions. Recent comparison of the measured structural and transport properties and computed band structure in $AuIn_2$ led to the conclusion that [12] an electronic topological transition (ETT) [13] occurs in it near 3 GPa followed by a structural phase transition near 9 GPa. For $AuAl_2$, only a structural transition is observed near 12 GPa [14]. Consistent with this, in $AuAl_2$, the computed electronic band structure had the flat band above the Fermi level at the ambient volume and hence no possibility of any electronic transition under pressure. $AuGa_2$ is an intermediate case, but no recent investigation aimed at this aspect is available. Here the results of electrical resistance (R), thermoelectric power (TEP), angle-dispersive x-ray diffraction (ADXRD) measurements and the first principles band structure calculations under pressure carried out on $AuGa_2$ are presented and discussed.

2. Experimental details

$AuGa_2$ was prepared by arc melting appropriate amounts of the components in a copper hearth under argon atmosphere. Characterization of the samples by x-ray diffraction under ambient conditions yielded a lattice parameter ($A = 6.079$ Å, space group $Fm3m$) in agreement with the literature value [15].

3. Transport measurements

For thermoelectric power measurements up to 10 GPa, an opposed Bridgman anvil apparatus was used with Pyrophyllite gaskets for pressure containment, and steatite (talc) for pressure transmission. Thin sheets of the materials of approximate size 3 mm × 5 mm with a thickness of 0.2 mm were prepared by cutting the material which had been flattened by pressing small chips between tungsten carbide anvils. For TEP measurements, alumel and chromel thermocouple wires were used. A nichrome heater was used to maintain temperature gradient along the sample. The details of the sample assembly and measurements are given elsewhere [16].

Electrical resistance measurements were carried out up to 19 GPa employing a clamp type Merrill Bassett diamond anvil cell (DAC) with a diamond culet size of 400 μm and a stainless steel gasket. Myler embedded alumina that results in quasi-hydrostatic conditions [17] was used as the pressure-transmitting medium. The pressure was measured by the ruby fluorescence technique. Measurements were carried out on a small rectangular piece of the sample (thickness $\sim$5 μm) kept at the centre of the anvil face and touching the leads. Full details of the techniques are given elsewhere [17].

4. ADXRD measurements

Synchrotron-based ADXRD measurements were carried out at Elettra. The powdered sample along with silver or platinum as pressure calibrant was loaded in a modified Mao-Bell [18] type diamond anvil cell in a hardened stainless steel or tungsten–tantalum alloy gasket with 100 μm gasket hole. Methanol:ethanol was used as the pressure-transmitting medium. The Elettra experimental station is based on an imaging plate area detector. X-ray powder patterns at various pressures were collected employing x-rays of wavelength 0.687 96 Å or 0.750 534 Å (calibrated values for two separate runs). The data were collected with typical exposure time of 15 min at each pressure. The scanned two-dimensional diffraction patterns were corrected for detector tilt and were collapsed to one-dimensional patterns using standard FIT2D software [19].

5. Band structure calculations

The total energy calculations were performed using the full potential linear augmented plane wave method (FP-LAPW), as implemented in the WIEN2K computer program [20]. This is based on density functional theory and is first principle in nature with only the atomic number of the elements as input. The errors in this approach are limited to the approximation of the exchange–correlation energy functional, cut-offs in the expansion of the basis functions, **k**-point sampling in the integrations over the Brillouin zone, and Born–Oppenheimer approximation. In the FP-LAPW method there is no approximations as regards the crystal geometry; the charge density and potential can have arbitrary shape though the wavefunctions are only variational approximations of the true wavefunctions in the region of fixed energies E_v. The calculation is fully relativistic for the core states but semi-relativistic with second variational treatment of spin–orbit coupling for the valence states. For the exchange–correlation terms the generalized gradient approximation (GGA) [21] was used. Muffin-tin radii (R_{mt}) of two Bohr units were employed for both Au and Ga. The desired precision in the total energy is achieved by using a plane wave cut-off $R_{mt}K_{max} = 9$ and a **k**-point sampling in the Brillouin zone (BZ) of 5000 points.

6. Results and discussions

In the following, we first discuss the results of band structure calculations and relate the anomalous behaviour of $AuGa_2$ to occupied states close to Fermi level in the Γ–X direction. The structural and transport properties are examined in the light of the pressure-induced electronic topological transitions seen in the band structure under compression.

Figure 1(a) shows the electronic band structure of $AuGa_2$ at the ambient volume without spin–orbit coupling. It is clear from the figure that a flat band exists in the Γ–X direction of the BZ, close to ($\sim$0.4 eV below) the Fermi level at ambient pressure, consistent with earlier calculations [5]. Inclusion of spin–orbit coupling retains the flatness of this band but its

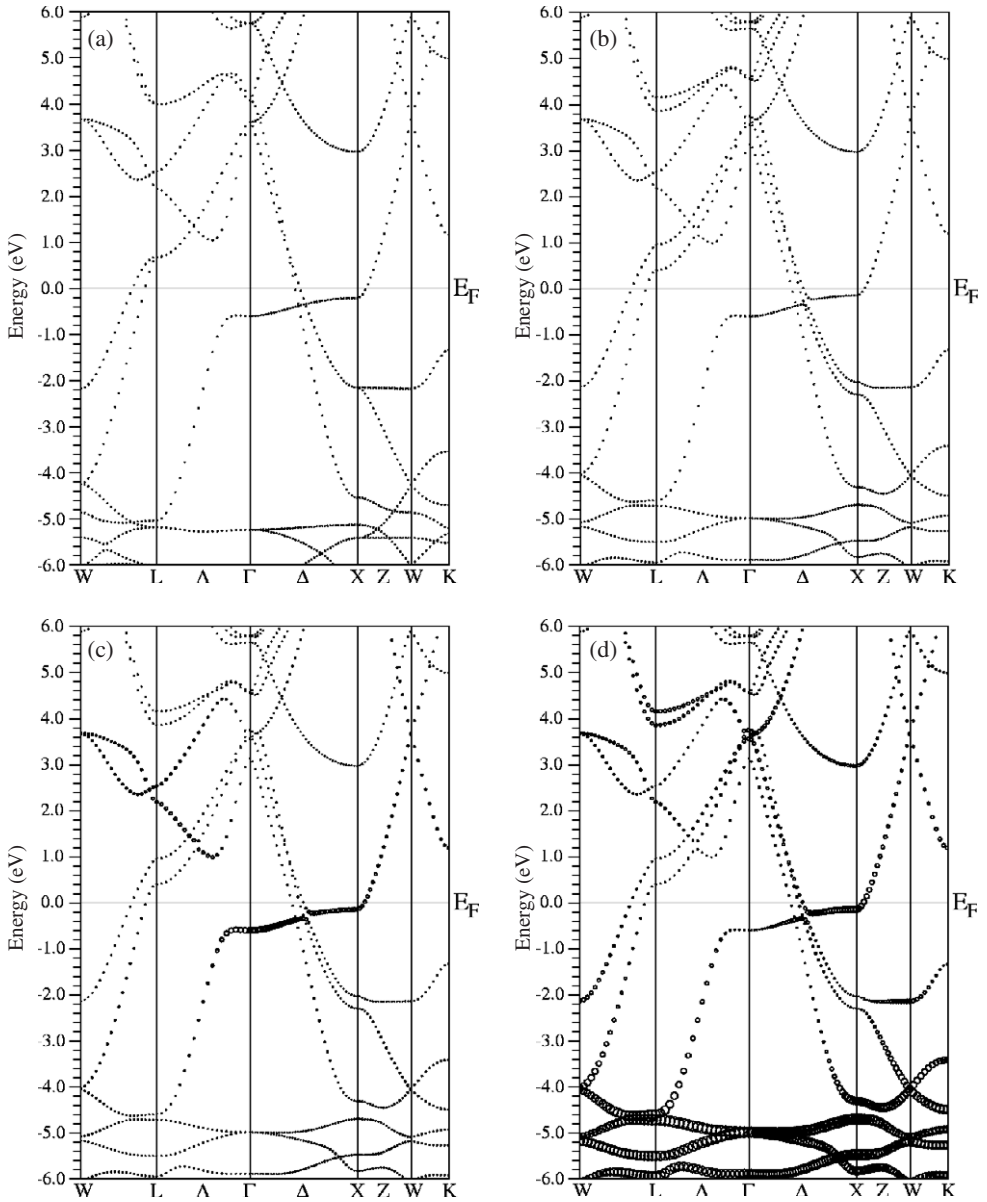

Figure 1. (a) Energy band structure at ambient volume without spin–orbit coupling. (b) Energy band structure at ambient volume with spin–orbit interactions. ((c) and (d)) Energy band structure at ambient volume with spin–orbit interactions. The 'flat band' representations that show the character of band (for the Ga 4p and Au 5d states, respectively) are employed. The size of the symbols is proportional to the character of Ga 4p (Au 5d) states. Note that the flat band in the Γ–X direction mainly have the Ga 4p and Au 5d character and is close to the Fermi level.

connectivity near the mid-point of Γ–X gets changed (leading to a gap as shown in figure 1(b)) due to hybridization with a more dispersive band (which was doubly degenerate in the non-relativistic limit; the degeneracy gets lifted due to the spin–orbit term). This flat band in the Γ–X direction is mainly a mixture of Au 5d and Ga 4p states (and not Ga s suggested in earlier

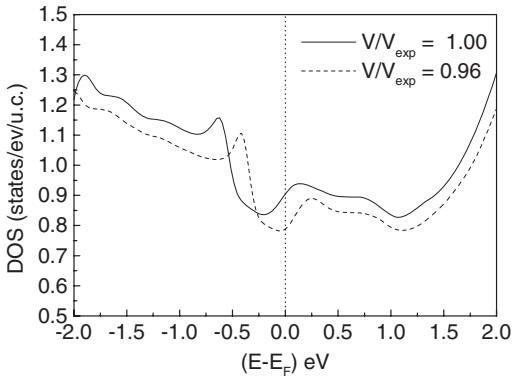

Figure 2. The total density of states (DOS) per eV in the unit cell at ambient volume and at a volume compression of 4%.

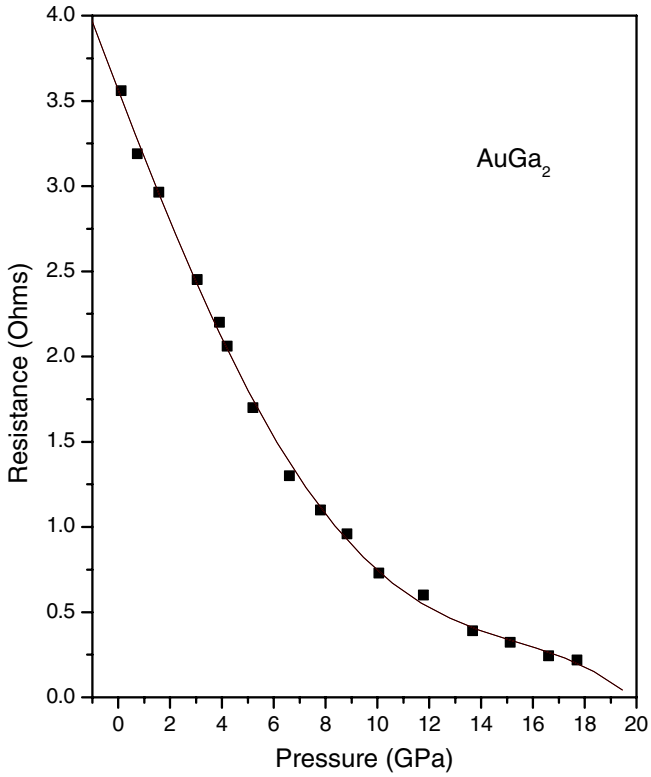

Figure 3. Pressure variation of electrical resistance up to 18 GPa measured in the diamond anvil cell.

calculations [5]), as shown in the figures 1(c) and (d). The change in connectivity due to spin–orbit term, however, has little effect on the ETT occurring at the X-point of the BZ. The density of states obtained by the band structure calculations is shown in figure 2.

The pressure variation of electrical resistance of $AuGa_2$, shown in figure 3, exhibits a continuous decrease up to 19 GPa. The TEP shown in figure 4 shows continuous increase with

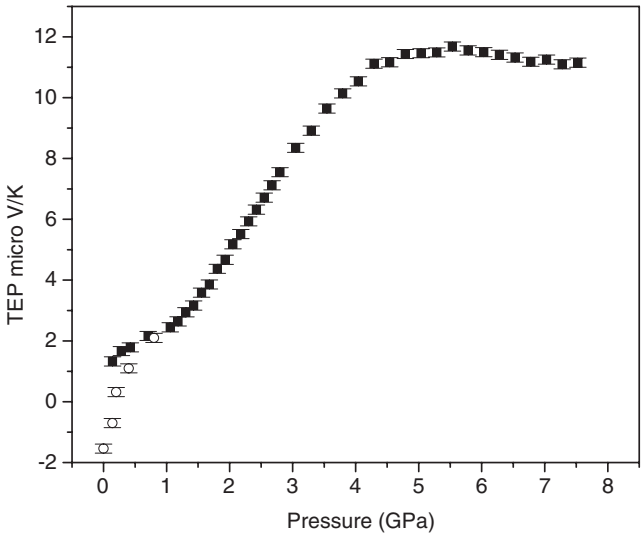

Figure 4. Pressure variation of the TEP for $AuGa_2$. In the low-pressure region, results of two separate measurements are plotted to confirm the change in sign of the TEP. The estimated measurement error in the TEP is also indicated.

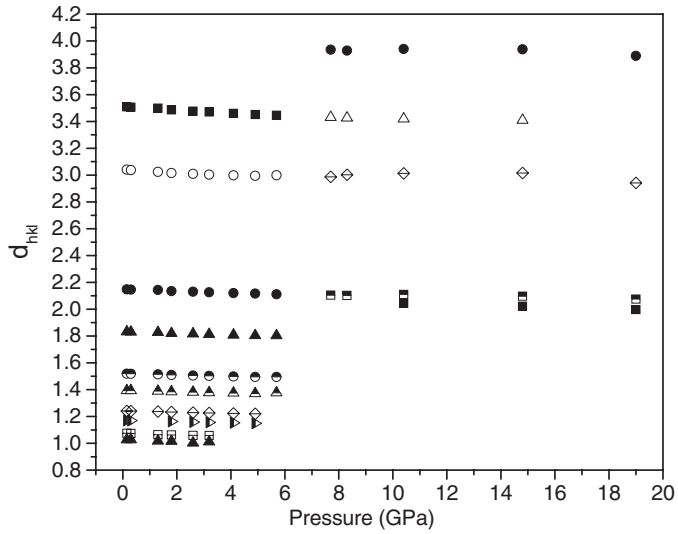

Figure 5. The variation of d-values with pressure. The close relation between the ambient CF_2 structure and the orthorhombic high-pressure phase is clear.

pressure from a low negative value ($-1.0\ \mu V\ K^{-1}$) and exhibits saturation above 4 GPa. The TEP has changed sign close to ambient pressure. Although the resistance data do not show any anomalous behaviour which would indicate a structural or iso-structural transition, the continuous increase and the saturation of the TEP does indicate the presence of an electronic rearrangement or a subtle structural transition near 4 GPa. The evolution of d-values as a function of pressure is shown in figure 5. The diffraction patterns do not show any structural phase transition until 7 GPa, ruling out the cause of saturation in the TEP as due to a structural

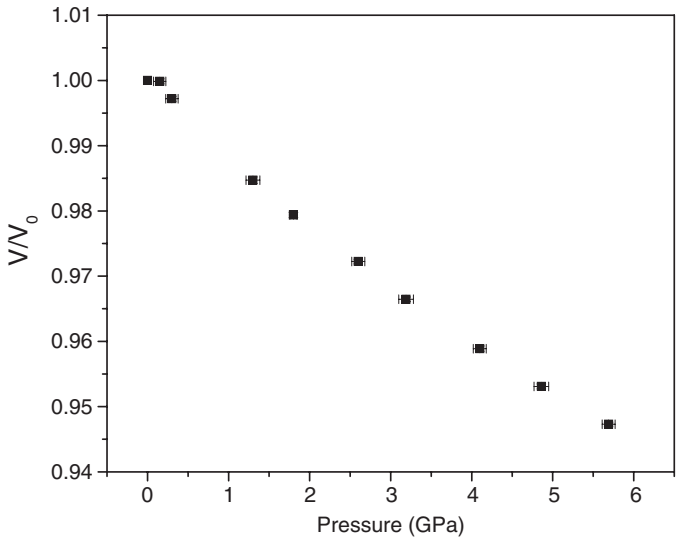

Figure 6. P–V data for $AuGa_2$ fitted to the Birch–Murnaghan equation of state. The estimated error in P and V is also indicated.

transition near 4 GPa. The calculated total density of states indicates the presence of a valley near the Fermi level, and with compression of 4%, the Fermi level shifts towards the valley (see figure 2). This feature accounts for the changes in the sign of the TEP with temperature variation as the sign of the electronic contribution (diffusion term) to the TEP for s–p metals is decided by the energy derivative of the density of states at the Fermi level and can change with the relative shift of the Fermi level.

In figure 6 we show the measured P–V data for $AuGa_2$ up to 7 GPa. The P–V data when fitted to Birch–Murnaghan equation of states (BM EOS) give the value of bulk modulus as 98 GPa with the pressure derivative kept fixed at 4. This is close to the value of 100 GPa estimated from the elastic constant measurements [4].

The universal equation of state, UEOS, [$\ln H = \ln B_0 + \eta(1 - X)$] expressed in the scaled variables H and X [$H = PX^2/3(1 - X)$ and $X = (V/V_0)^{1/3}$, with V_0, ambient volume, V volume at pressure P, and $\eta = 3(B_0' - 1)/2$, where B_0' is the pressure derivative of the bulk modulus B_0] is linear in the absence of any electronic and structural transition [22]. Thus subtle changes accompanying an electronic transition that are not perceptible in the P–V curve will be seen as a deviation from linearity in the universal equation of state (UEOS) [22]. The measured P–V data on $AuGa_2$ converted to the scaled parameters of the universal equation of state (figure 7) clearly show a change of slope near 3.2 GPa. Thus P–V data indicate the possibility of an ETT near 3.2 GPa in $AuGa_2$. In the investigations on Cd and Zn [23], the role of non-hydrostatic pressure on c/a anomalies associated with the subtle electronic transitions are widely investigated. In $AuGa_2$, since the anomaly occurs far away from the freezing point of the ethanol–methanol mixture, these effects are expected to be minimal.

As the presence of an ETT will also be discernable in the pressure variation of the electronic structure, the electronic structure calculations were carried out at a volume compression of $V/V_0 = 0.96$ corresponding to an estimated pressure of 4 GPa (figure 8). It is clear that the flat band in the Γ–X direction of the BZ, which is just below (∼0.4 eV) the Fermi level at ambient pressure, moves up and touches the Fermi level near 4 GPa at the X-point of the BZ (figure 8). Thus the evolution of band structure with pressure confirms the presence

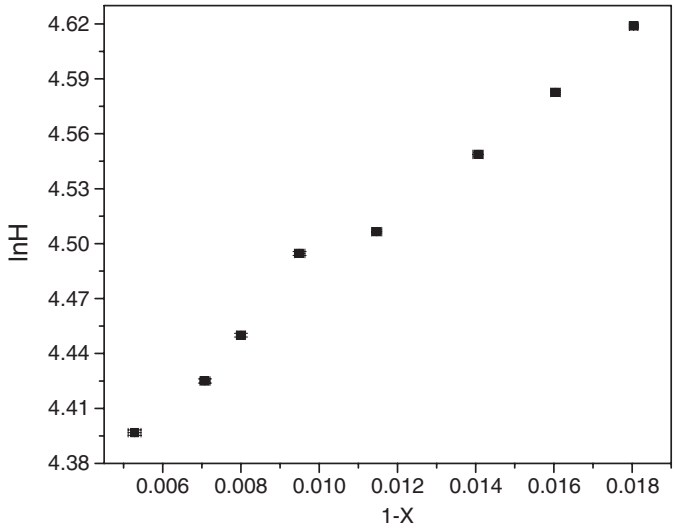

Figure 7. UEOS for $AuGa_2$. It shows a clear discontinuity at 3.2 GPa. The estimated error is also indicated.

Table 1. The orthorhombic indexing of the $AuGa_2$ pattern at 10.4 GPa. ($a = 11.200$ Å, $b = 4.3105$ Å, $c = 4.2116$ Å.)

d_{obs}	d_{cal}	h	k	l
3.9453	3.9421	1	0	1
3.4251	3.4158	2	1	0
3.0126	3.0124	0	1	1
2.6485	2.6529	2	1	1
2.1129	2.1164	1	2	0
		0	0	2
2.0485	2.0509	4	1	1
1.8695	1.8667	6	0	0
		1	1	2

of an ETT in $AuGa_2$. Earlier Fermi surface measurements have indicated the occurrence of an electronic transition near 0.6 GPa at low temperature [24]. The small volume change required or the effect of thermal depopulation may be the reason why the transition pressures at low temperature and ambient temperature are different.

Above 7 GPa the changes in the diffraction pattern indicate the presence of a structural phase transition. The high-pressure pattern up to 10 GPa could be fitted to a low-symmetry orthorhombic phase (table 1) closely related to the cubic phase ($A_o = 2A_c$, $B_o = \sqrt{2}A_c$ and $C_o = \sqrt{2}A_c$). This structure continuously evolves as the pressure is increased, as indicated by the continuous change in intensity and pressure shift of the diffraction peaks. This behaviour of diffraction lines implies a transition to a structure closely related to CaF_2 type, by distortion. However, because of the continuous evolution of the XRD patterns in intensity as well as in the axial ratio, the complete structural details (space group, atom positions) could not be obtained. It may be noted that on further compression above 4 GPa, the second part of the flat band will also cross the Fermi level at a point mid-way along the Γ–X direction. This crossing may be driving this structural transition.

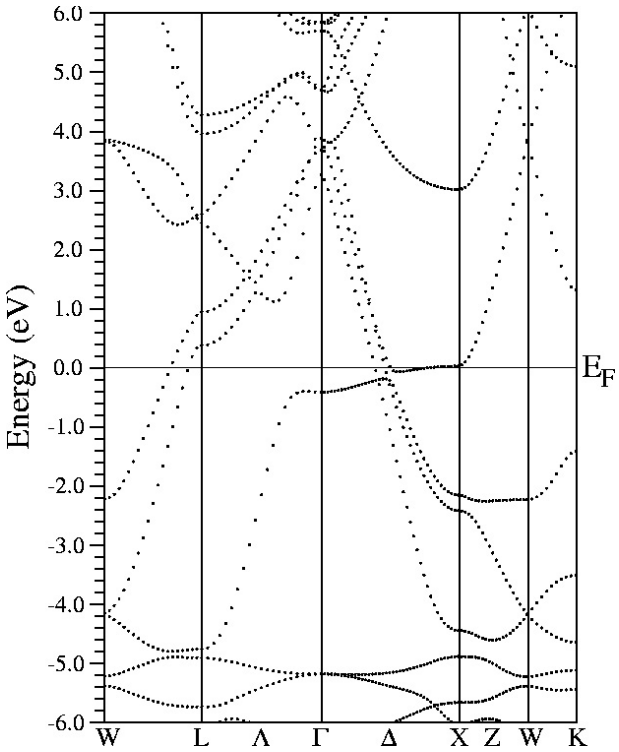

Figure 8. The band structure at 4% compression. A flat band close to the Fermi level along the Γ–X direction crosses it under compression.

7. Conclusions

The results of x-ray diffraction and transport measurements show the presence of an ETT near 3.2 GPa and are consistent with the fusion data. The first principles electronic structure calculation corroborates these experimental findings. Also, beyond 7 GPa a structural transition is observed. The high-pressure data could be fitted to a low-symmetry orthorhombic phase closely related to the CaF_2 phase. The present work thus confirms that the anomalous ambient and high-pressure behaviour of $AuGa_2$ is due to the presence of a flat band very close to the Fermi level.

Acknowledgments

We sincerely thank Dr A Lausi and Dr E Bussetto for all the help during measurements at Elettra. ABG and VVK thankfully acknowledge the ICTP for travel support and hospitality at Elettra. The x-ray diffraction measurements were carried out under proposal No. 1999389.

References

[1] Jan J-P and Pearson W B 1963 *Phil. Mag.* **8** 279
[2] Jaccarino V, Weger M, Wernick J H and Menth A 1968 *Phys. Rev. Lett.* **21** 1811
[3] Jaccarino V, Blumberg W E and Wernick J H 1961 *Bull. Am. Phys. Soc.* **6** 104
[4] Testardi L R 1970 *Phys. Rev.* B **1** 4851

[5] Switendick A C and Narath A 1969 *Phys. Rev. Lett.* **22** 1423
Kim S, Nelson J G and William R S 1985 *Phys. Rev.* B **31** 3460
Gupta A and Sengupta R 1991 *Phys. Status Solidi* b **168** 455
[6] Hsu L S, Denlinger J D and Allen J W 1998 *Mater. Res. Soc. Symp. Proc.* **524** 179
Nelson J G, Gignac W J, Kim S, Lince J R and Williams R S 1985 *Phys. Rev.* B **31** 3469
[7] Hsu L S, Wang H W, Tai Y-L and Lee J-F 2005 *Phys. Rev.* B **7** 115115
Hsu L S, Huang H W and Tsang K L 1998 *J. Phys. Chem. Solids* **59** 1205
Sham T K 1987 *Solid State Commun.* **64** 1103
[8] Hahn E and Seraphin B O 1978 *Phys. Thin Film* **10** 1
[9] Lince J R and Williams R S 1985 *J. Vac. Sci. Technol.* A **3** 1217
Lince J R and Williams R S 1986 *Thin Solid Films* **137** 251
[10] Bosch W P, Chinchure A, Flokstra J, de Groot M J, Van Heumen E, Jochemsen R, Mathu F, Peruzzi A and Veldhuis D http://www.xs4all.nl/~hdleiden/srd1000/reports/srd1000.doc
[11] Storm A R, Wernick J H and Jayaraman A 1966 *J. Phys. Chem. Solids* **27** 1227
[12] Godwal B K, Jayaraman A, Meenakshi S, Rao R S, Sikka S K and Vijayakumar V 1998 *Phys. Rev.* B **57** 773
Godwal B K, Meenakshi S, Modak P, Rao R S, Sikka S K, Vijayakumar V, Bussetto E and Lausi A 2002 *Phys. Rev.* B **65** R140101
[13] Lifshitz I M 1960 *Sov. Phys.—JETP* **11** 1130
Dagens L 1978 *J. Phys. F: Met. Phys.* **8** 2093
[14] Garg A B, Verma A K, Vijayakumar V, Rao R S and Godwal B K 2005 *Phys. Rev.* B **72** 024112
[15] Pearson W B 1967 *Handbook of Lattice Spacing and Structures of Metals and Alloys* vol 2 (Oxford: Pergamon)
[16] Singh A K and Ramani G 1978 *Rev. Sci. Instrum.* **49** 1324
[17] Garg A B, Vijayakumar V and Godwal B K 2004 *Rev. Sci. Instrum.* **75** 2475
[18] Vijayakumar V and Meenakshi S, BARC/2000/I/014
[19] Hammersley A P, Svensson S O, Hanfland M, Fitch A N and Hausermann D 1996 *High Pressure Res.* **14** 235
[20] Blaha P, Schwarz K, Madsen G K H, Kvasnicka D and Luitz J 2001 *WIEN2K, An Augmented Plane Wave + Local Orbitals Program for Calculating Crystal Properties* ed K Schwarz (Austria: TU Wien)
[21] Perdew J P, Burke K and Ernzerhof M 1996 *Phys. Rev. Lett.* **77** 3865
[22] Sikka S K 1988 *Phys. Rev.* B **38** 8463
[23] Pratesi G, Di Cicco A, Minicucci M and Itie J P 2005 *J. Phys.: Condens. Matter* **17** 2625
Kenichi T 1999 *Phys. Rev.* B **60** 6171
[24] Abele J C, Brewer J H and Halloran M H 1971 *Solid State Commun.* **9** 977